Figure

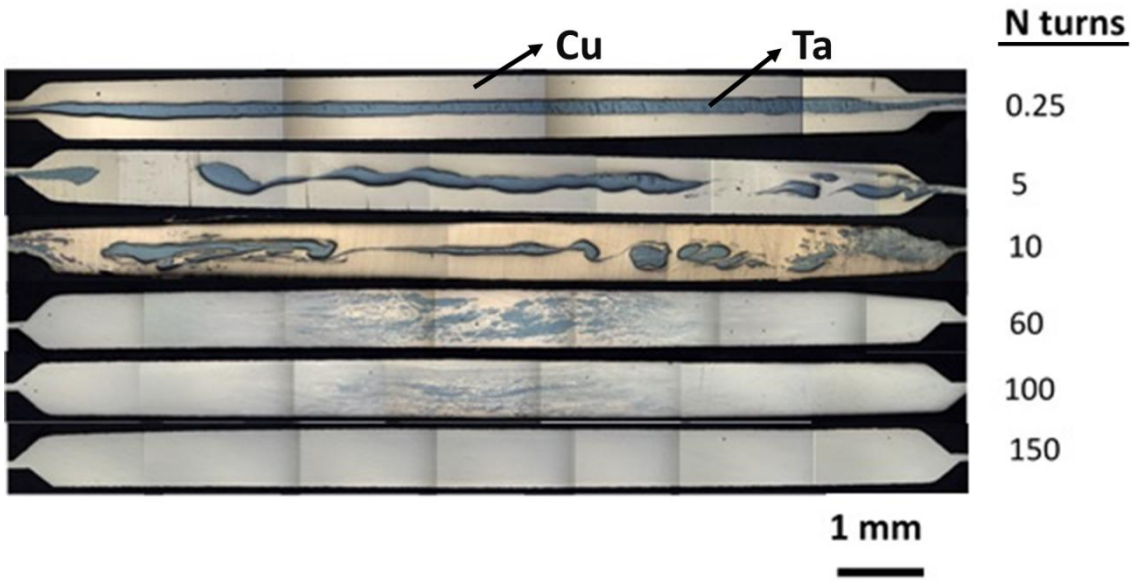

Fig. 1 Cross-sectional OM images of Cu/Ta/Cu stacks after different numbers of HPT turns: the dark regions are Ta and the bright regions are Cu.

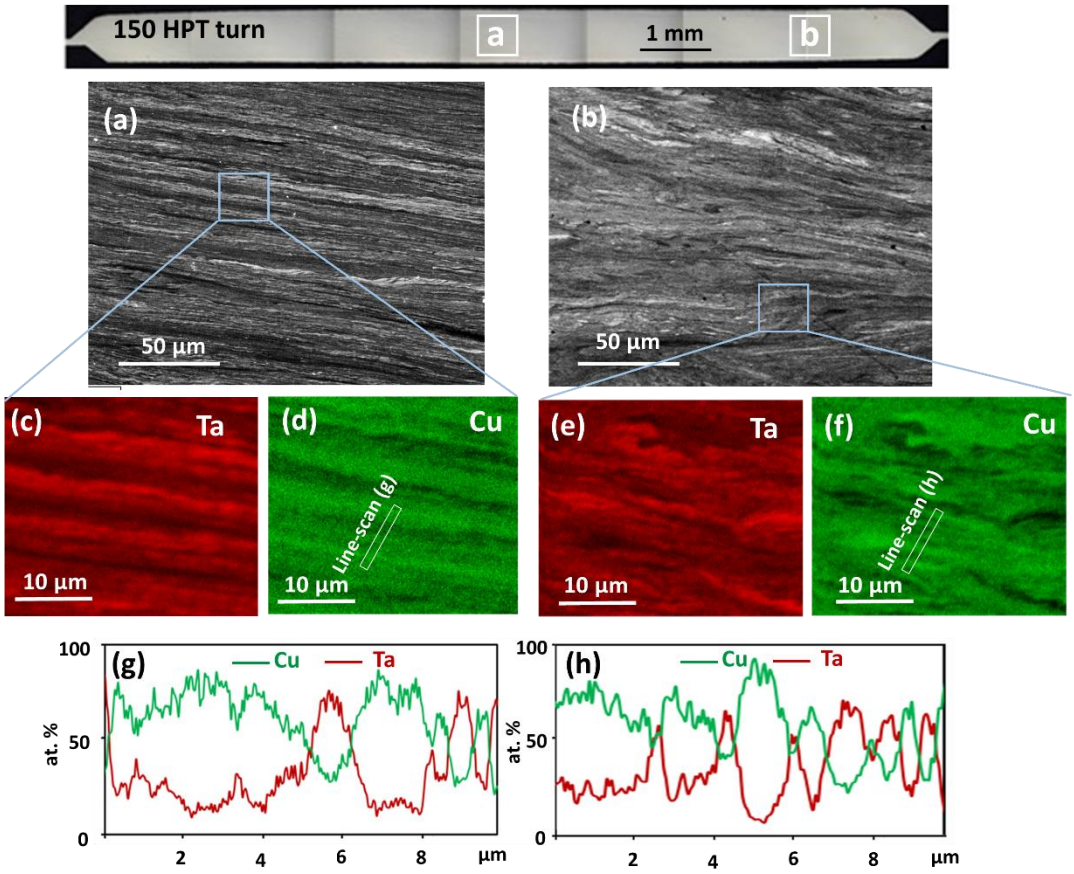

Fig. 2 Cross-sectional SEM images of the 150 turns sample at the areas marked (a) in the centre and (b) near the edge area, (c-f) elemental Cu and Ta maps of the indicated regions at higher magnifications, (g,h) EDX line scans over the region marked in d and f.

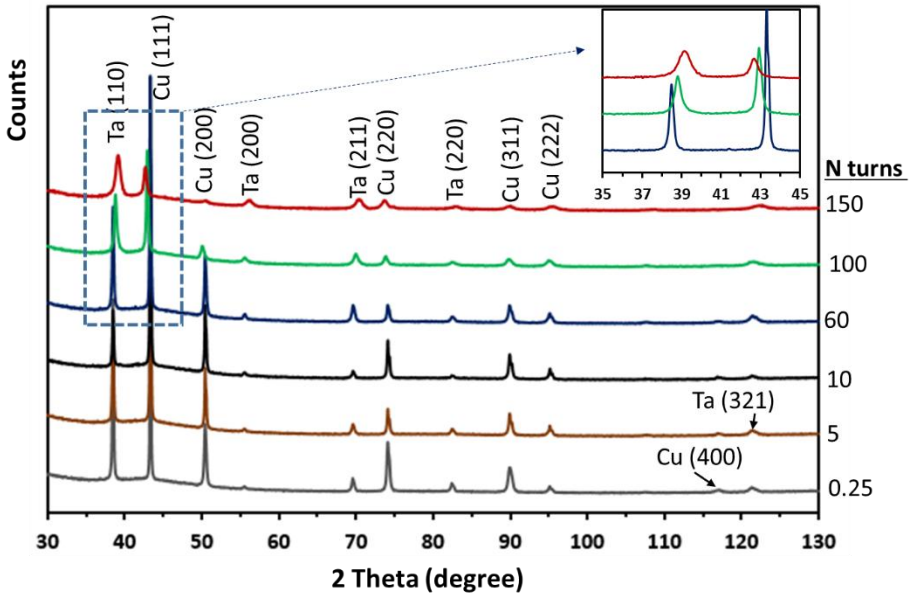

Fig. 3 The XRD patterns of the Cu-Ta discs processed by HPT at different numbers of turns (0.25, 5, 10, 60, 100 and 150). The inset shows the peak shifts for the Cu (111) and Ta (110) peaks after 100 turns.

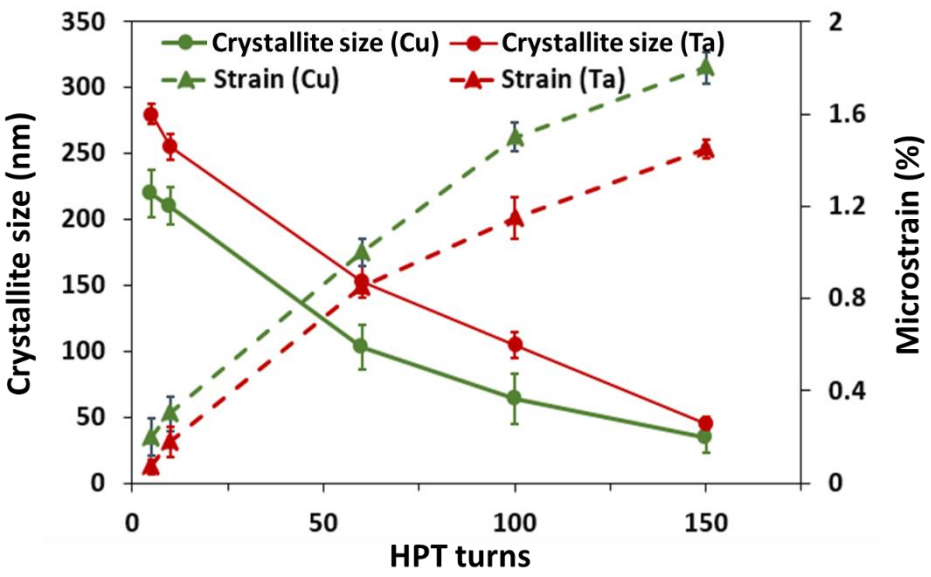

Fig. 4 Crystallite size and lattice strain in Cu and Ta at various HPT turns.

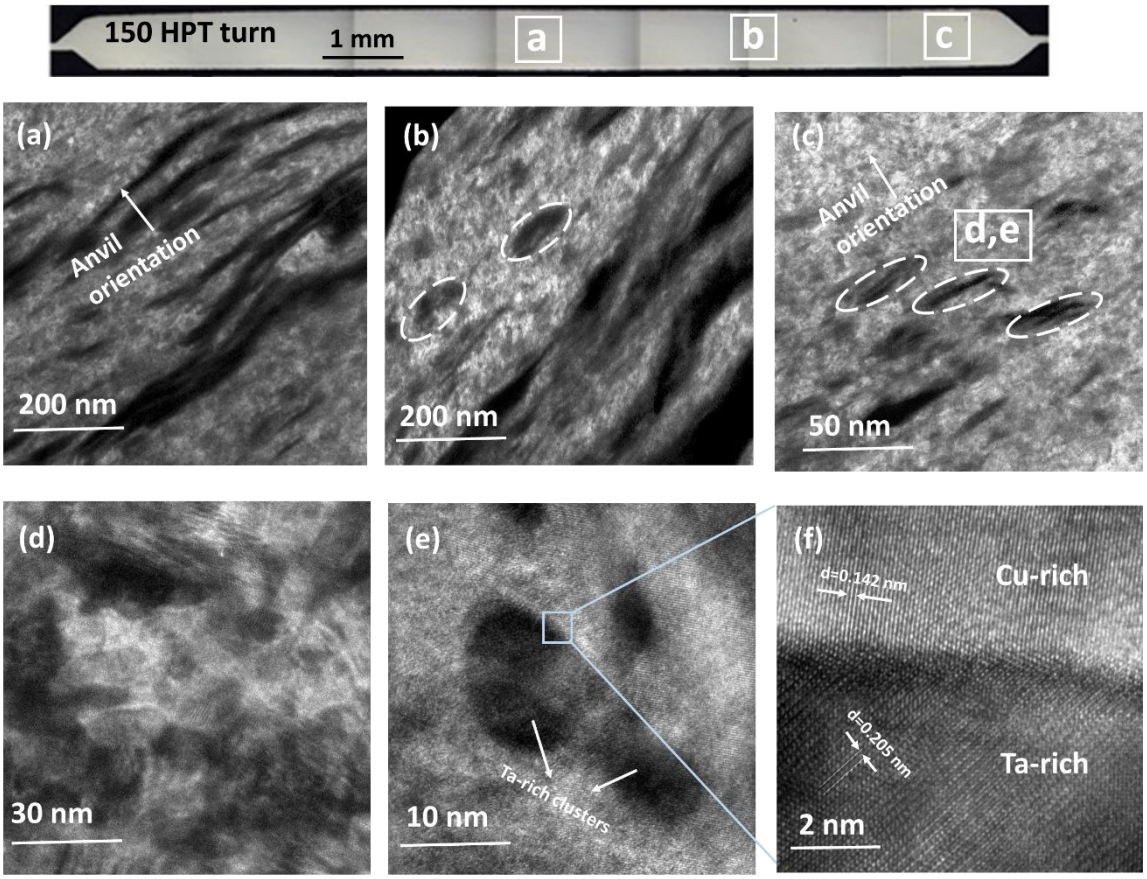

Fig. 5 (a-c) TEM images of the Cu-Ta bulk after 150 HPT turns at different positions through the disc as indicated, (d,e) high magnification image of the matrix at the edge area and (f) atomic resolution TEM image of the interface between a Ta-rich area and the Cu-rich matrix.

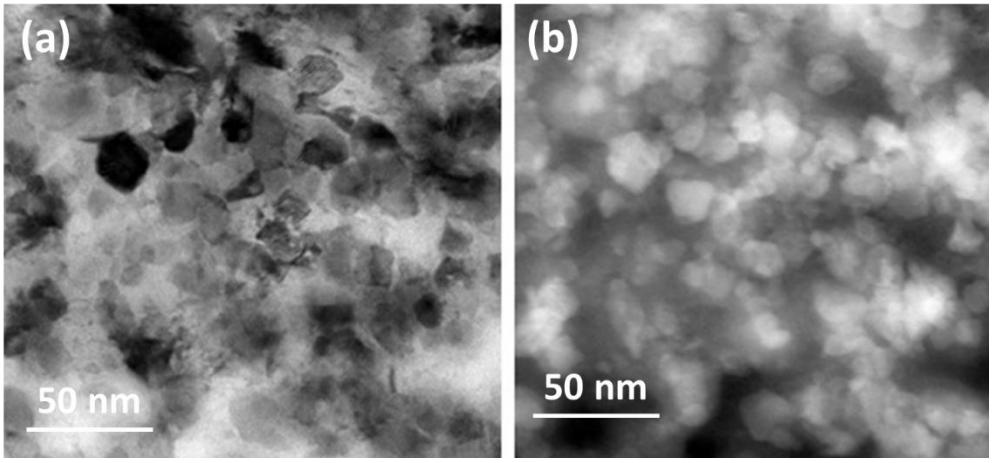

Fig. 6 (a) STEM and (b) Z-contrast HAADF images of Cu-Ta sample after 150 HPT turns.

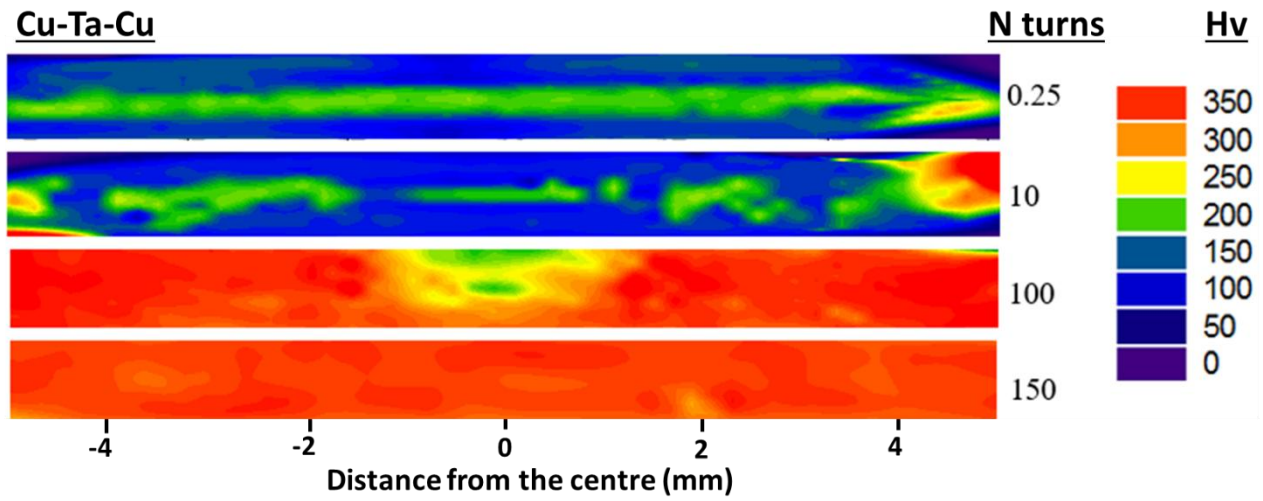

Fig. 7 Colour-coded microhardness maps of the Cu/Ta/Cu stacks after different numbers of HPT turns.

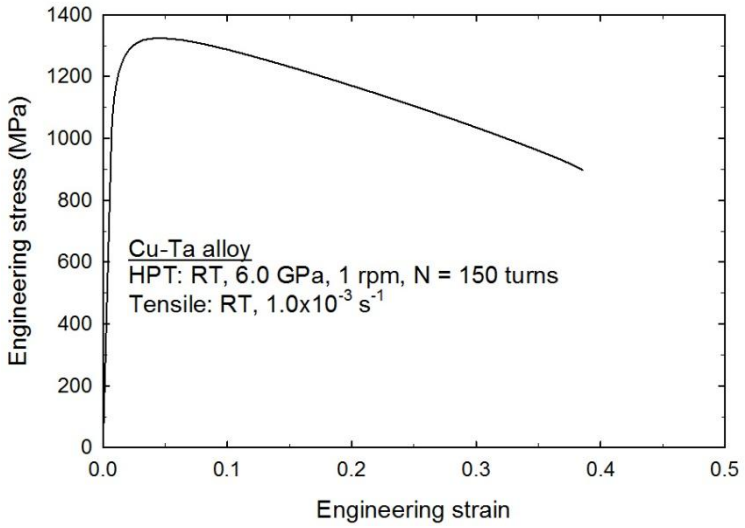

Fig. 8. Stress-strain curve for the Cu-Ta bulk sample after processing through 150 HPT turns.

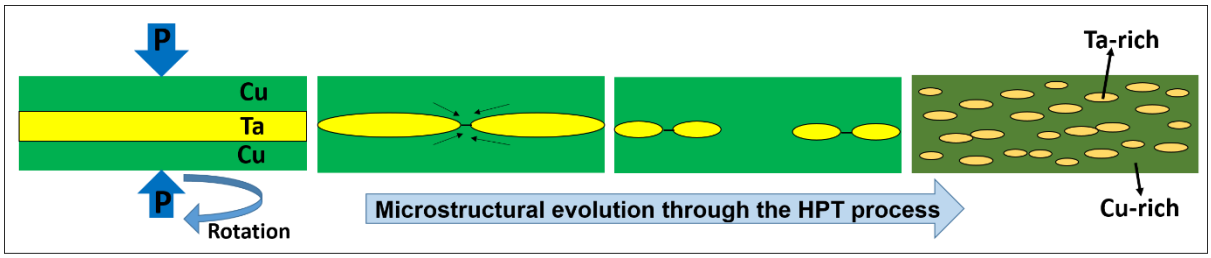

Fig. 9 Schematic image illustrating the mechanism of microstructural evolution in the Cu-Ta bulk through HPT processing.